CALIBRATION OF THE HYPERVELOCITY IMPULSE TUNNEL

OCTOBER 1963
DOUGLAS REPORT SM-43060

MISSILE & SPACE SYSTEMS DIVISION
DOUGLAS AIRCRAFT COMPANY, INC.
SANTA MONICA CALIFORNIA

DOUGLAS

(6) 268 700

CALIBRATION OF THE HYPERVELOCITY IMPULSE TUNNEL,

(11) OCTOBER 1963
DOUGLAS REPORT SM-43060

(12) (14)

PREPARED BY: J.A. COPPER and
F.J. HAMEETMAN

PREPARED UNDER THE SPONSORSHIP OF
THE DOUGLAS AIRCRAFT COMPANY
INDEPENDENT RESEARCH AND
DEVELOPMENT PROGRAM.
ACCOUNT NO. 80450-287/55247

J.F.L. Aldrich

APPROVED BY:
J.F.L. ALDRICH
BRANCH CHIEF
ENGINEERING R&D LABORATORIES

RESEARCH AND DEVELOPMENT SUPPORT DEPARTMENT
MISSILE & SPACE SYSTEMS DIVISION
DOUGLAS AIRCRAFT COMPANY, INC.

SUMMARY

The Hypervelocity Impulse Tunnel (HIT) is a versatile, high-performance shock tunnel located at the Douglas Aerophysics Laboratory (DAL). This shock tunnel uses the tailored-interface and equilibrium-interface techniques to provide test durations of at least 10 milliseconds. These test durations are sufficiently long to enable forces and pressures as well as heat-transfer rates to be measured.

Results of the calibration of the test section of the HIT are presented. Flow uniformity and repeatability, inviscid core size, the effects of reservoir pressure, reservoir enthalpy level, and test-section axial location are discussed. Velocities up to 17,000 ft/sec, test section Mach numbers between 8.1 and 22.6, and Reynolds numbers between 2.5×10^3 and 4×10^6 per foot have been observed. It is believed that the velocity performance can be increased to 20,000 ft/sec by utilizing the equilibrium-interface technique with a combustion driver. Further, it is believed that the Mach number range can be extended from 8.0 to 24.0 and the Reynolds number range can be extended from 2×10^2 to 10^7 per foot by appropriate changes in the reservoir pressure level.

Pressure and heat transfer distributions on simple bodies have been measured at nominal Mach numbers of 9 and 23, respectively. These investigations are interpreted according to appropriate aerothermodynamic theory and are compared with data from other facilities.

TABLE OF CONTENTS

1.0 INTRODUCTION

A complete description of the Hypervelocity Impulse Tunnel (fig. 1) may be found in reference 1. Basically, the shock tunnel operates like a very short-duration, blowdown wind tunnel. A shock tube is used to process the test air to a stagnant, high-pressure, high-enthalpy state. This reservoir gas is then expanded through a nozzle to a hypersonic Mach number in the test section. By using the tailored-interface technique (ref. 2) test durations of at least 10 milliseconds are obtained.

The testing region in the HIT is within the free jet that issues from the 30-inch-diameter conical nozzle. This nozzle utilizes interchangeable throat inserts to vary the expansion area ratio. The test section conditions depend on the tunnel reservoir conditions as well as the nozzle area ratio because of real-gas and boundary-layer effects.

The conceptual simplicity and flexibility of the shock tunnel make it possible to obtain broad ranges of aerodynamic flow properties in the test section. Since it is not practical to calibrate the HIT over its entire operating envelope, two sets of operating conditions (designated "hot" and "cold") have been defined which should encompass nearly all conditions of interest.

When operating under "hot" conditions, the total flight enthalpy at a given Mach number is duplicated while under "cold" operation only enough enthalpy to avoid condensation of the airstream is provided. The "hot" condition is appropriate to problems where real gas effects are important while the "cold" condition permits higher Mach numbers and yields higher Reynolds numbers at a given Mach number and pressure level.

The test section of the HIT has been calibrated at both operating conditions for each of the three nozzle throats presently available. The techniques used and the results of this calibration are presented below.

2.0 SYMBOLS

h	enthalpy
M	Mach number
M_s	shock Mach number; the speed of a shock wave relative to the gas into which it is propagating divided by the sound speed in that gas
p	pressure
q	heat-transfer rate
r	radius
R	radius of inviscid core or body radius
s	distance along body from stagnation point
t	time
T	temperature
x	distance, either from shock tube diaphragm or nozzle entrance
X	distance aft of nozzle exit
γ	ratio of specific heats
θ	nozzle half angle

Subscripts and Superscripts

R	reservoir
t	total conditions
1	state of gas initially in driven tube
5	state of gas behind the reflected shock wave
$*$	Mach number one
$'$	behind normal shock wave

3.0 THEORETICAL PERFORMANCE ESTIMATES

An estimate of conditions expected in the test section can be made by assuming one-dimensional, isentropic nozzle flow in chemical equilibrium and making a suitable correction for boundary-layer growth. The semi-empirical method of reference 3 is considered to be the best available method for predicting turbulent boundary-layer growth. Predictions of test section Mach number and inviscid core radius based on references 3 and 4 are shown in figures 2 - 4.

The conditions shown on figures 2 - 4 are at the nozzle exit. However, because of the radial nature of the flow generated by the conical nozzle, one would expect an axial Mach number gradient at the nozzle exit. Neglecting boundary-layer effects, this axial gradient can be expressed as

$$\frac{dM}{dx} \approx (\gamma-1) \left(\frac{\gamma+1}{\gamma-1}\right)^{\gamma+1/4} \left(\frac{r^*}{x\theta}\right)^{2-\gamma} \frac{\theta}{r^*} \qquad (1)$$

The Mach number gradients calculated from Eq. (1) for the 0.840-, 0.120-, and 0.030-inch-diameter throats are 0.35, 0.76, and 1.33/ft, respectively.

4.0 EXPERIMENTAL ARRANGEMENT

4.1 Reservoir Conditions

One of the great advantages of the shock tunnel is that the reservoir conditions can be accurately determined. The reservoir pressure p_5 and enthalpy h_5 are calculated from the shock tube initial conditions, p_1 and T_1, and the incident shock Mach number M_s, all of which can be measured quite accurately.

The shock speed was measured in the standard fashion by measuring its transit time between known points. Either thin-film resistance thermometers (ref. 5) or ionization probes (ref. 5) were used to detect the shock wave. When thin-film resistance thermometers were used the gage outputs were fed through high-gain pulse amplifiers into electronic counters. The ionization gage outputs do not require amplification.

The initial pressure in the driven tube was measured with a 60-inch mercury manometer. The air, before diaphragm burst, was assumed to be at the same temperature as the shock tube.

The reservoir pressure was monitored with two pressure transducers (Kistler Model 605). One transducer was mounted in the shock-tube end wall and the other was mounted in the shock-tube sidewall, one inch upstream of the end wall (directly opposite the nozzle entrance). The outputs from these transducers were fed into charge amplifiers (Kistler Model 565) and then were recorded on an oscilloscope. In addition, the transducer outputs were often filtered electronically. Measured reflected shock pressures, p_5, usually agreed with the calculated values of p_5 to within 5 percent. Typical reservoir pressure records for each operating point are shown in figure 5.

4.2 Test Section Measurements

An impact or pitot-pressure distribution across the test section was taken on all runs during the test section calibration program. The pitot probes were bolted to a strut (fig. 6) which was bolted to the test section floor. The probes could be moved continuously in the vertical centerplane and axially in four-inch increments (with probe extensions). A cross rake (also shown in fig. 6) was used to survey the flow out of the vertical centerplane.

Pressures were sensed with piezoelectric pressure transducers. Both transducers developed at the DAL and those commercially available were used. When Kistler or Atlantic Research Corporation transducers were used, it was necessary to shock mount the transducers to minimize their acceleration response. At reservoir enthalpy levels above about 1500 Btu/lb gas radiation from the stagnation point caused the level of pyroelectric (thermal) output to become comparable to the piezoelectric (pressure) signal. Shielding was provided by using a slanted port so that the transducer could not "see" the high energy gas.

The homemade DAL transducer was designed to minimize thermal response as well as acceleration response. All transducers were calibrated by employing a quick-opening gate valve to generate a step input* of pressure. The homemade DAL transducers and the calibration technique are described in more detail in reference 6.

---

*The rise time of this pressure pulse is about 2 milliseconds.

On several runs, attempts were made to verify two assumptions: (1) that the test section enthalpy actually was the same as the reservoir enthalpy, and (2) that the test section enthalpy actually was constant during the time of constant reservoir pressure. The first assumption is necessary if M is to be calculated from p_t'/p_R assuming isentropic nozzle flow. The second assumption is especially questionable if the equilibrium-interface technique is to be used. To investigate the first assumption the stagnation-point heat-transfer rate was measured and the enthalpy determined from boundary-layer theory (ref. 7). A calorimeter (Hidyne Model HT-10 or HT-100) was used to measure the heat-transfer rate. To investigate the second assumption the output versus time of a calorimeter or of a cold-wire probe (similar to that described in ref. 8) was investigated. Platinum wires about one inch long and between 0.001 and 0.003 inch in diameter were used as the cold-wire probe. Figure 7 shows some typical test section oscillograms.

5.0 CALIBRATION RESULTS

5.1 0.840-Inch-Diameter Throat/Cold Operation

For this operating point a driver gas mixture of cold helium and nitrogen, chosen to yield tailored-interface conditions at a shock Mach number of about 2.8, was used. A typical reservoir pressure record (fig. 5a) shows that the usable test duration (time of uniform reservoir conditions) is over 20 milliseconds. A corresponding pitot-pressure record is shown in figure 7a.

Figure 8 shows a vertical airflow distribution for this operating point obtained 7-1/2 inches aft of the nozzle exit. Five runs are included so that the repeatability as well as the uniformity is illustrated. The average Mach number M is 11.0 with a variation of ± 0.2. The free-stream velocity is 5040 ft/sec, the free-stream temperature is 85°R, and the inviscid core radius is slightly less than 12 inches. For these runs the predictions from figure 2 are M = 11.4 and R = 10.9 inches. Thus, in this case the method of reference 3 overestimates the boundary-layer thickness but underestimates its displacement thickness.

The observed axial Mach number gradient and effect of reservoir pressure on Mach number are illustrated in figure 9. There it is seen that Eq. (1) gives a satisfactory estimate of the axial Mach number gradient and that the effect of reservoir pressure on Mach number is indeed small, as figure 2 predicts.

Stagnation point heat-transfer rates were measured with calorimeters during two runs. The stagnation enthalpies calculated using these

results and the theory of reference 7 were about 10% higher than the reservoir enthalpies calculated from the measured shock speed. This agreement is within the usual accuracy of experiments and the Fay-Riddell theory. More important though, as shown in figure 7a, the heat-transfer rate remained constant during the test duration indicating that the stagnation enthalpy also remained constant.

5.2 0.840-Inch-Diameter Throat/Hot Operation

For this operating point a cold hydrogen driver gas is used and tailored-interface conditions are obtained near $M_s = 6.0$. A typical reservoir pressure record (fig. 5b) shows a usable test duration of 14 milliseconds. The dip and subsequent recovery in reservoir pressure during the first 1.5 milliseconds is a phenomena associated with combustion at the hydrogen-air interface.

A vertical airflow distribution obtained 7-1/2 inches aft of the nozzle exit is shown in figure 10. Five different runs with a reservoir pressure of about 850 psi and a reservoir enthalpy of about 1950 Btu/lb are included. For these runs the Mach number was 9.04. The free-stream velocity was 9520 ft/sec, the free-stream temperature was about $460^{\circ}R$, and the inviscid core radius was nearly 11 inches. Again, figure 2 overestimates the Mach number slightly and slightly underestimates the inviscid core radius.

Figure 11 illustrates the effects of distance from the nozzle exit, reservoir pressure level, and reservoir enthalpy level on the free-stream Mach number. Theoretical predictions obtained by cross-plotting the results from figure 2 are also included. Since the Mach number predictions from figures 2 - 4 do not agree with the experimental values the curves crossplotted from figures 2 - 4 are shifted closer to the experimental points to facilitate comparison. Figure 11 shows that the axial gradient is slightly larger than predicted by Eq. (1). The observed effect of pressure level is slightly larger than predicted from figure 2 and the effect of reservoir enthalpy level is adequately predicted by figure 2.

5.3 0.120-Inch-Diameter Throat/Cold Operation

The reservoir conditions for this operating point can be conveniently generated by two methods. A cold mixture of hydrogen and nitrogen picked to yield tailored-interface conditions at a shock Mach number of about 4.8 is one possibility. However, for this case, combustion at the driver-driven gas interface is experienced. Another possibility is to use a cold helium driver gas and use the equilibrium-interface technique (ref. 9). Both driver modes were tried and both gave satisfactory results. Typical reservoir pressure records are shown in figures 5c and 5d. Figure 7c is an oscillogram of the output of a calorimeter mounted in the test section during an equilibrium-interface run. The constant slope indicates a constant heat-transfer rate and consequently a constant stagnation enthalpy level.

A vertical airflow distribution obtained 1/2 inch forward of the nozzle exit is shown in figure 12. Three different runs with a reservoir pressure of about 1040 psi and a reservoir enthalpy level of about 1550 Btu/lb are included. For these runs the Mach number was about 17.3, the free-stream velocity was 8500 ft/sec, the free-stream temperature was $104^{\circ}R$, and the inviscid core radius was about 6 inches. For this case figure 3 provides a good estimate of the Mach number but underestimates the inviscid core considerably. Figure 13 illustrates the effects of distance from the nozzle exit, reservoir pressure level and reservoir enthalpy level on the free-stream Mach number. The axial Mach number gradient is less than that computed from Eq. (1). This can be explained by the more rapid boundary-layer growth experienced when using this throat which tends to cut down the effective nozzle cone angle.

The three experimental points on the M versus h_R plot indicate a larger effect of h_R on M (by about a factor of two) than is expected from figure 3. Since the free-stream temperature T for the two higher M points is about $50^{\circ}R$, condensation is a possible explanation.

Consider the behavior of the pitot pressure p_t' as the total temperature T_t (or reservoir enthalpy) is decreased (for a fixed nozzle expansion ratio) from the point where condensation effects are first noticed. Daum (ref. 10) shows that the p_t' first increases then decreases as T_t is decreased. Thus the two higher M points could be explained if they are in the T_t range where p_t' has fallen below its before-condensation value. However Daum's data indicates that the T where condensation effects would first be noticeable (an increase in p_t') is below $30^{\circ}R$ for the range of conditions being considered here. Hence condensation must be ruled out.

Another consideration is that the two higher M points were obtained with a hydrogen-nitrogen driver gas mixture and equilibrium-interface operation while the lower M point was obtained with a helium driver and equilibrium-interface operation. Now the computation of h_R for either of these operating conditions is not completely obvious (ref. 11). In both cases h_R was computed by assuming isentropic processes between reflected-shock and reservoir conditions. The h_R for the equilibrium-interface condition might be expected to be lower than computed (if the driver gas cools the air reservoir) while h_R for the hydrogen-nitrogen drive might be expected to be higher than computed (if the combustion at the interface does not affect the reservoir enthalpy level). Such changes in h_R would only make the experimental points differ from the predictions by a greater amount. For these reasons, it is thought that the experimental points describe the actual flow and, for some reason that is not clear, the effect of h_R on M is considerably larger than expected for this particular operating point.

Pressure level has an increased effect on Mach number as the throat diameter decreases; the observed effect of pressure level is predicted well by figure 3.

5.4 0.120-Inch-Diameter Throat/Hot Operation

The reservoir conditions for this operating point are generated by using a combustible mixture to produce tailored-interface conditions near $M_s = 8.0$. Here the combustible mixture is a stoichiometric

mixture of hydrogen and oxygen, diluted with 84.5% helium. A typical reservoir pressure oscillogram is shown in figure 5e. There it is seen that the usable test duration is about 10 milliseconds and the disturbance associated with combustion at the interface is still present even though all of the hydrogen should have been consumed by the driver combustion process. Figure 7b is an oscillogram of the test section pitot pressure illustrating the uniformity of test section conditions with the combustion drive.

A vertical airflow distribution obtained 7-1/2 inches aft of the nozzle exit is shown in figure 14. The reservoir pressure of 3595 psi and reservoir enthalpy of 3805 Btu/lb produce a test section Mach number of 14.1 with a velocity of 13,600 ft/sec and a free-stream temperature of 386°R. The inviscid core radius is slightly over six inches. Thus, for this operating condition, figure 3 overestimates the Mach number by about 5% and slightly underestimates the core radius.

The effects of distance from the nozzle exit, reservoir pressure, and reservoir enthalpy level on M are illustrated in figure 15. Again the axial Mach number gradient is less than that computed from Eq. (1). For this case the experimental points agree very well with the theoretical performance estimates cross-plotted from figure 3.

5.5 0.030-Inch-Diameter Throat/Cold Operation

This operating point also uses a cold hydrogen driver. A vertical airflow distribution obtained 7-1/2 inches aft of the nozzle exit with a reservoir pressure of about 3500 psi is shown in figure 16. The Mach number is about 23 but it is apparent that the usable core of inviscid flow has a diameter of only two or three inches. Since

it was felt that this usable test core would not be sufficient for many model tests, no more calibration was attempted at this operating point.

5.6 0.030-Inch-Diameter Throat/Hot Operation

This operating point uses a combustion driver that is more energetic than the one previously described. A mixture with the nominal molar composition of 8 helium : 3 hydrogen :1oxygen was used. This mixture enables tailored-interface conditions to be obtained at $M_s = 10$ and should permit equilibrium interface conditions up to about $M_s = 11.7$.

An attempt to determine the vertical airflow distribution with a reservoir pressure of 2500 psi showed that the usable test core was about two inches in diameter, and the Mach number obtained was about 16. Because of the small core, no additional calibration was attempted.

6.0 SUMMARY OF TEST SECTION FLOW SURVEY

The results of the flow surveys in the test section with the three different throat inserts have been tabulated in Table I. This table shows the range of reservoir conditions where actual calibration has been accomplished and the range of test section Mach numbers obtained. All Mach numbers are at the nozzle exit. Also included are the ranges of inviscid core diameter, and Reynolds number per foot attained.

7.0 EXPERIMENTAL RESULTS ON SIMPLE MODELS

7.1 Pressure Distribution on Hemisphere-Cylinder Model

A three-inch-diameter hemisphere-cylinder model (fig. 17) was instrumented with homemade piezoelectric pressure transducers and tested at the hot condition with the 0.840-inch-diameter throat. Pressure orifices were located at values of s/R of 0.523, 1.050, 1.740, and 2.580. Oscillograms of typical transducer outputs are shown in figure 18.

The data obtained are compared with data obtained on a similar body in shock tubes, continuous hypersonic wind tunnels, and hotshot wind tunnels in figure 19. The data from three runs fall within the symbol. It is seen that the data obtained in the HIT exhibits much less scatter than the shock-tube data and compares very favorably with the continuous wind tunnel data.

7.2 Heat Transfer Measurements on a Cylinder Model

A 3/4-inch-diameter pyrex test tube was instrumented with thin-film resistance thermometers and mounted transverse to the airflow. A schlieren picture of a similar but larger model in a Mach number 9 airflow is shown in figure 20. Two gages were located at the stagnation point and one was located 60 degrees around the body. This model was tested using the 0.030-inch-diameter throat at a nominal Mach number of 23. Oscillograms of the thin-film gage outputs are shown in figure 21.

Figure 22, which presents the variation in measured heat transfer rate with time, shows that the heat transfer rate is constant for four milliseconds. The heating rate then increases, presumably because of very small particles in the airstream.

The measurements at the stagnation point and at 60° agree with the theories of references 7 and 13, respectively, to within $\pm 2\%$. This close agreement must be considered slightly fortuitous because the accuracy of the heat transfer data is thought to be between 5 and 10 per cent.

8.0 CONCLUSIONS

The calibration of the test section of the HIT covered the Mach number range 8.1 to 22.6, the Reynolds number range 2.5×10^3 to 4×10^6 per foot, and the velocity range 5000 to 17,000 ft/sec. By increasing the reservoir pressure, it is believed that M can be increased to 24 and Re to 10^7 per foot. Velocities up to 20,000 ft/sec should be possible with a combustion drive and equilibrium-interface operation. Although M and Re cannot both be varied continuously with the three throats presently available, it is not difficult to fabricate new throat inserts. In fact, since the usable core is so small with the smallest throat, present plans are to fabricate a new throat which is somewhat larger.

The theoretical predictions presented in figures 2 - 4 overestimate the Mach number by about 5%. The predicted core diameters are off by between 1 and 2-1/2 inches; the predictions are low for the larger two throats and high for the small throat. The effects of p_R and h_R on M are predicted quite well from figures 2 - 4 with two exceptions which were noted.

The results of the pressure and heat transfer measurements on simple bodies are very encouraging. Combined with the airflow calibration results, they indicate that, in terms of flow uniformity, repeatability, and measuring techniques, the HIT compares favorably with other shock tunnels (e.g., Cornell Aeronautical Laboratory and General Electric). Further, the wide range of operating conditions of the HIT permits the generation of higher velocity airflows in chemical equilibrium than are possible in other hypervelocity wind tunnels.

9.0 REFERENCES

1. Copper, J. A., "The Hypervelocity Impulse Tunnel: Facility Description and Expected Performance," Douglas Aircraft Company, Inc. Report SM-41377 (November 1962).

2. Wittliff, C. E., Wilson, M. R., and Hertzberg, A. "The Tailored-Interface Hypersonic Shock Tunnel," J. Aerospace Sci. 26, 219-228 (1959).

3. Burke, A. F. and Bird, K. D. "The Use of Conical and Contoured Expansion Nozzles in Hypersonic Facilities," Advances in Hypervelocity Techniques (Plenum Press, New York, 1962), pp. 373-424.

4. Kaegi, E. M. and Warren, W. T., "Free Stream Properties of Argon-Free Air in Chemical Equilibrium for a One-Dimensional, Isentropic, Expansion Process," General Electric Report R61SD111 (December 1961).

5. Glass, I. I. and Hall, J. G., "Handbook of Supersonic Aerodynamics - Section 18 - Shock Tubes," NAVORD Report 1488 (Vol. 6)(December 1959).

6. Ogostalick, E. J., "Pressure Transducer Design, Fabrication, and Calibration at the Douglas Aerophysics Laboratory," Douglas Aircraft Company, Inc., Technical Memorandum (to be published).

7. Fay, J. A. and Riddell, F. R., "Theory of Stagnation Point Heat Transfer in Dissociated Air," J. Aeronaut. Sci. 25, 73-85 (1958).

8. Christiansen, W. H., "Development and Calibration of a Cold Wire Probe for Use in Shock Tubes," GALCIT Hypersonic Research Project Memo No. 62 (July 1961).

9. Copper, J. A., "Experimental Investigation of the Equilibrium Interface Technique," Phys. Fluids 5, 844-849 (1962).

10. Daum, F. L., "Air Condensation in a Hypersonic Wind Tunnel," AIAA J. 1, 1043-1046 (1963).

11. Copper, J. A., "Mixing and Combustion at the Interface in a Shock Tube," Douglas Aircraft Company, Inc., Engineering Paper No. 1795 (to be published).

12. Griffith, B. J. and Lewis, C. H., "A Study of Heat Transfer to Spherically Blunted Cones and Hemisphere-Cylinders at Hypersonic Conditions," AEDC-TDR-63-102 (June 1963).

13. Lees, L., "Laminar Heat Transfer over Blunt-Nosed Bodies at Hypersonic Flight Speeds," Jet Propulsion 26, 259-269 (1956).

TABLE I. SUMMARY OF CALIBRATION RESULTS

Nozzle Throat Diameter (inches)	Enthalpy Level	Reservoir Pressure P_R (psi)	Reservoir Enthalpy h_R (Btu/lb)	Mach Number M	Reynolds Number Re/ft (1/ft)	Inviscid Core Diameter (inches)
0.840	Cold	1000 - 4000	530	10.55	10^6 - 4×10^6	23
	Hot	565 - 3200	1740 - 2230	8.1 - 9.1	8.1×10^4 - 2.5×10^5	21
0.120	Cold	720 - 3185	985 - 1858	17.3 - 19.2	3.2×10^4 - 6.2×10^4	12
	Hot	970 - 3770	3150 - 4200	11.8 - 15.5	4.8×10^3 - 1.8×10^4	12
0.030	Cold	3170 - 3750	2000 - 2200	20.0 - 22.6	2.2×10^4	2
	Hot	2140 - 2760	4450	16	2.5×10^3	2

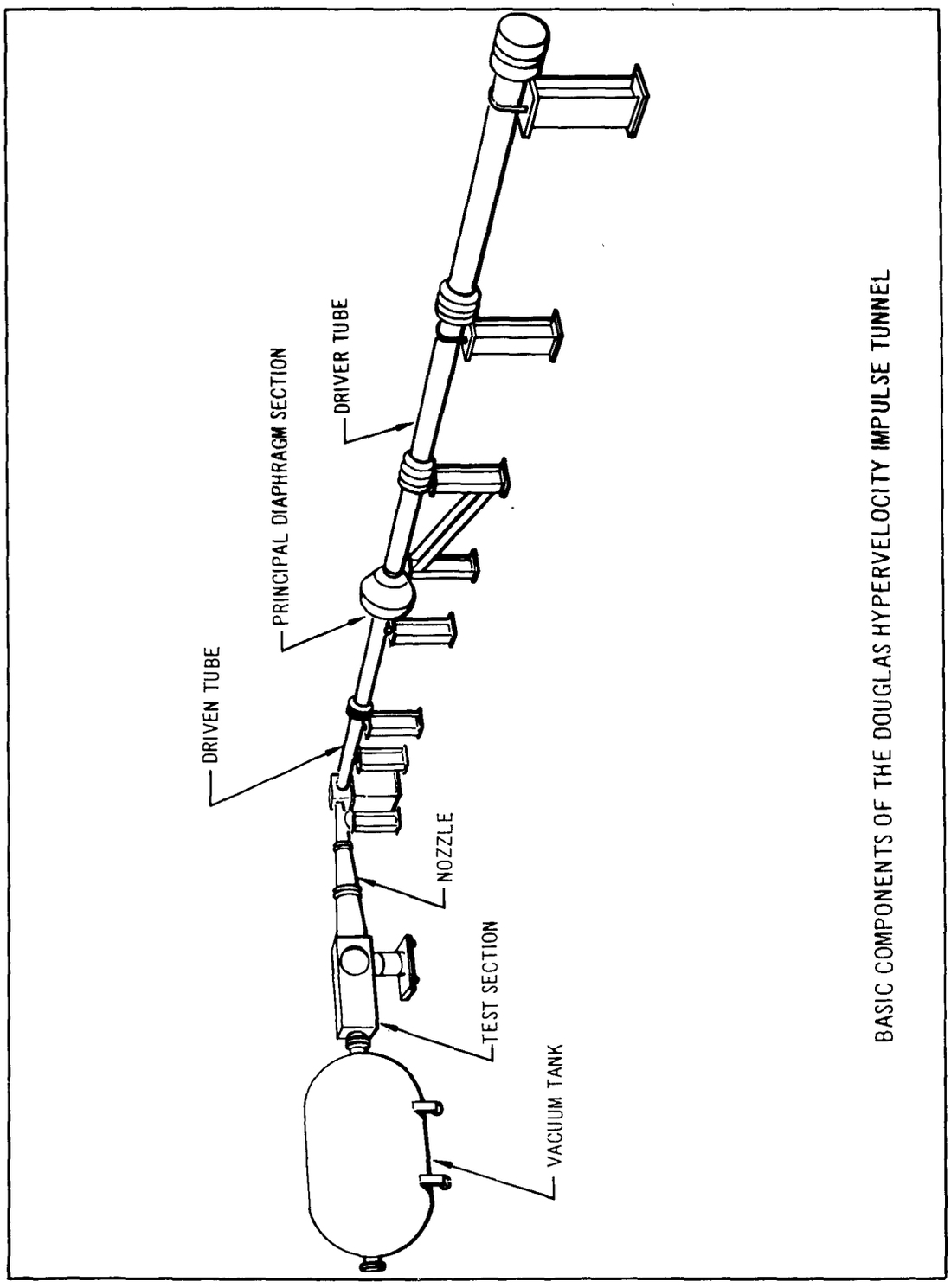
DRIVEN TUBE
PRINCIPAL DIAPHRAGM SECTION
DRIVER TUBE
NOZZLE
TEST SECTION
VACUUM TANK
BASIC COMPONENTS OF THE DOUGLAS HYPERVELOCITY IMPULSE TUNNEL

FIGURE 1

PERFORMANCE ESTIMATES -- 0.840-INCH-DIAMETER THROAT

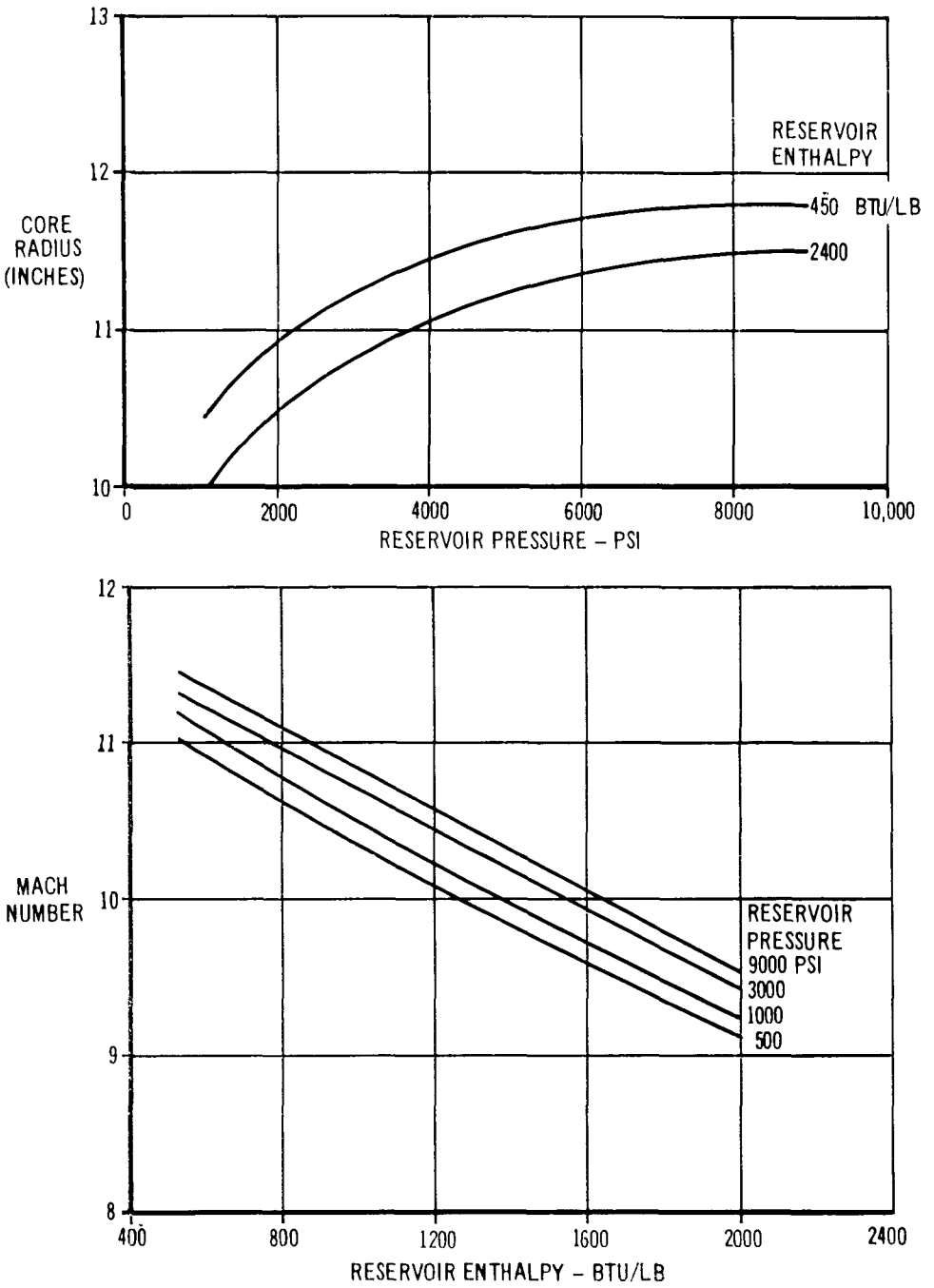

FIGURE 2

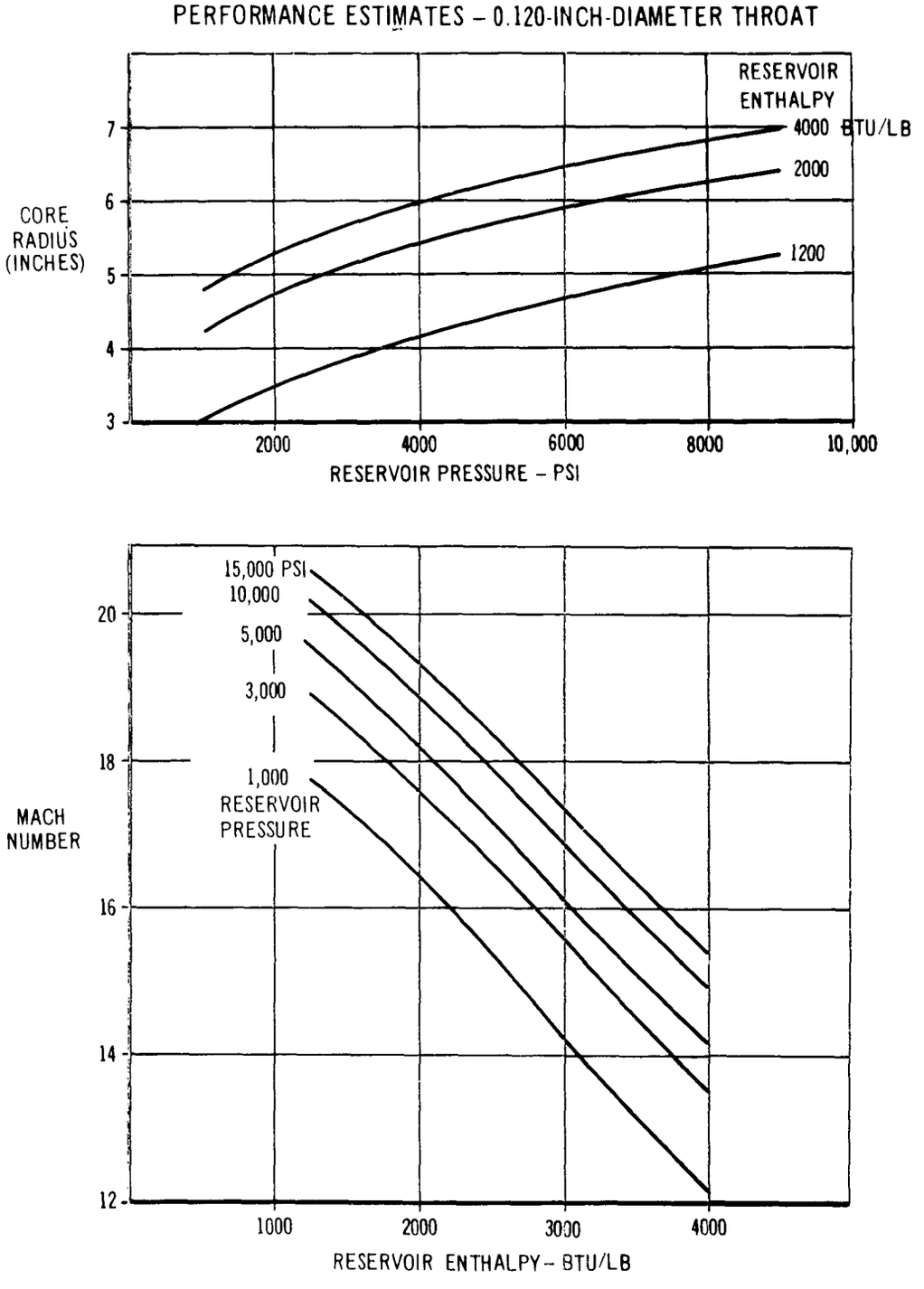
PERFORMANCE ESTIMATES – 0.120-INCH-DIAMETER THROAT
RESERVOIR ENTHALPY
4000 BTU/LB
2000
1200
CORE RADIUS (INCHES)
7
6
5
4
3
2000
4000
6000
8000
10,000
RESERVOIR PRESSURE – PSI
15,000 PSI
10,000
5,000
3,000
1,000
RESERVOIR PRESSURE
MACH NUMBER
20
18
16
14
12
1000
2000
3000
4000
RESERVOIR ENTHALPY – BTU/LB

FIGURE 3

PERFORMANCE ESTIMATES – 0.030-INCH-DIAMETER THROAT

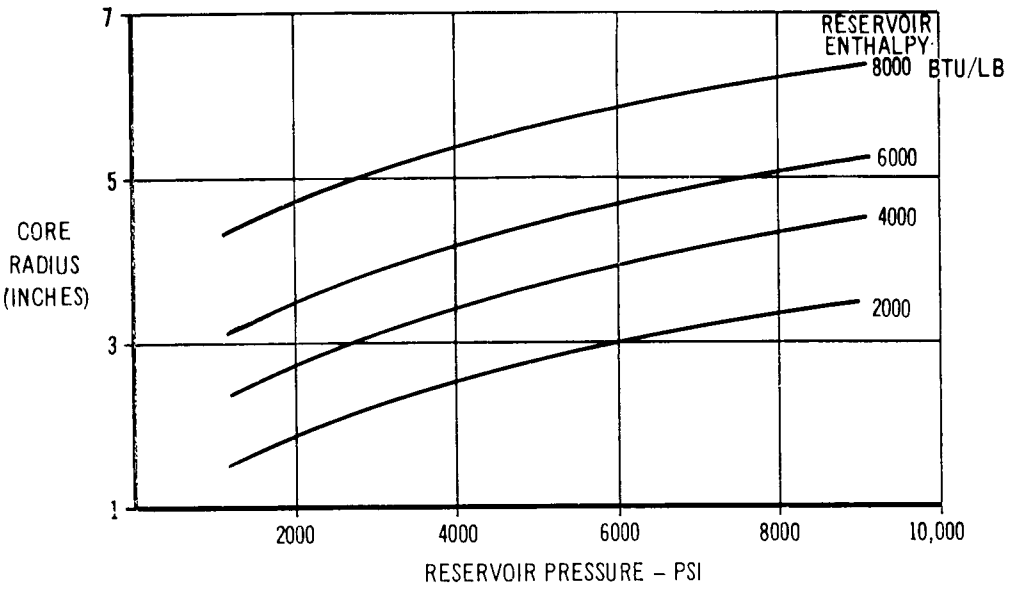

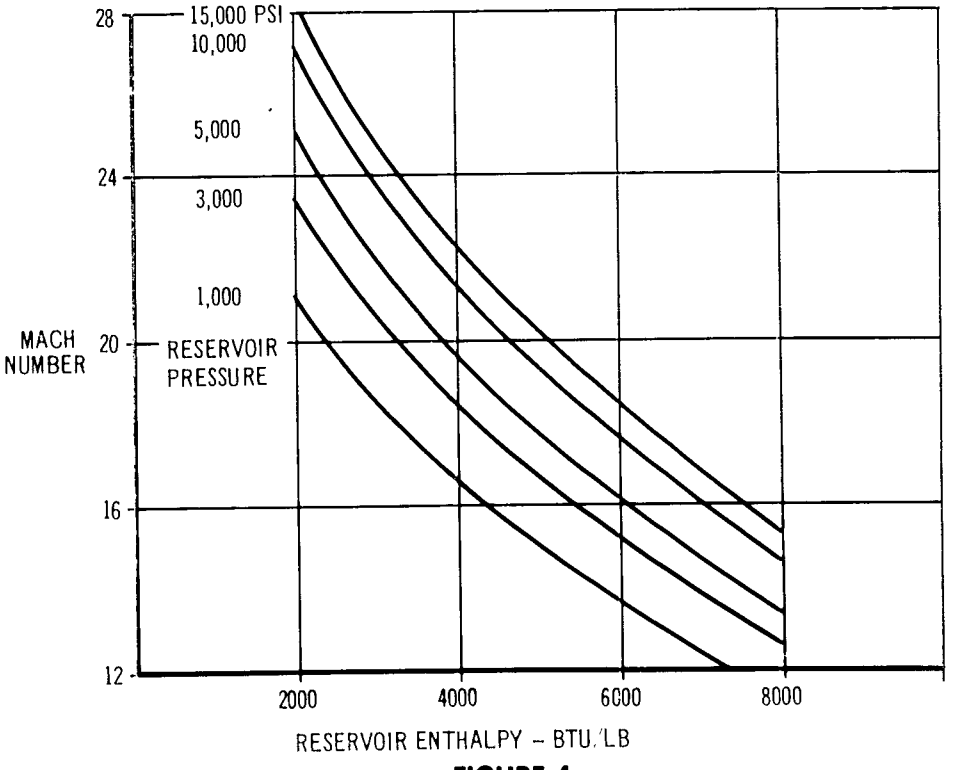

FIGURE 4

SHOCK TUNNEL RESERVOIR PRESSURE HISTORIES

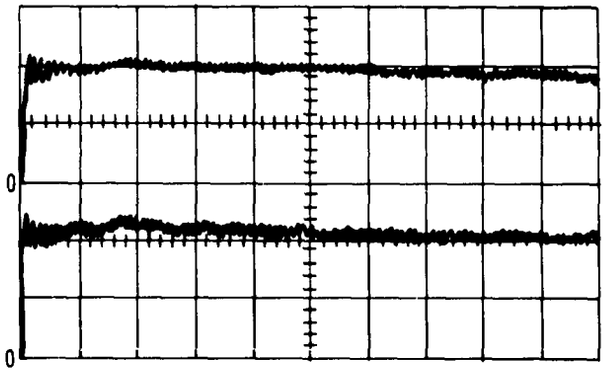

DRIVER GAS: HELIUM AND NITROGEN MIXTURE (M_S = 2.8)
SWEEP SPEED: 2 MILLISECONDS/DIVISION
VERTICAL SENSITIVITY: 1000 PSI/DIVISION

THE LOWER TRACES ARE ALL FILTERED ELECTRONICALLY.

FIGURE 5a

SHOCK TUNNEL RESERVOIR PRESSURE HISTORIES

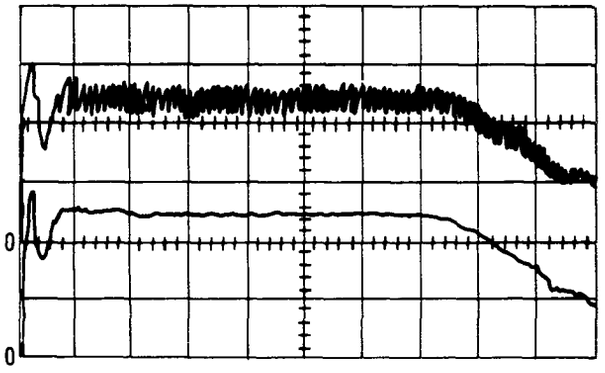

DRIVER GAS: HYDROGEN ($M_S = 6.0$)
SWEEP SPEED: 2 MILLISECONDS/DIVISION
VERTICAL SENSITIVITY: 400 PSI/DIVISION

FIGURE 5b

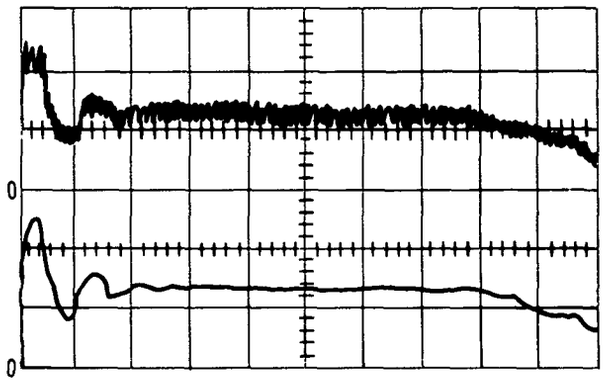

DRIVER GAS: HYDROGEN AND NITROGEN MIXTURE ($M_S = 4.5$)
SWEEP SPEED: 2 MILLISECONDS/DIVISION
VERTICAL SENSITIVITY: 1000 PSI/DIVISION

FIGURE 5c

SHOCK TUNNEL RESERVOIR PRESSURE HISTORIES

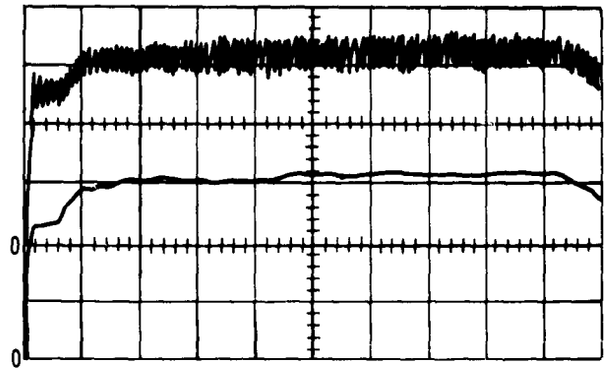

DRIVER GAS: HELIUM (M_S 4.8)
SWEEP SPEED: 2 MILLISECONDS/DIVISION
VERTICAL SENSITIVITY: 300 PSI/DIVISION

FIGURE 5d

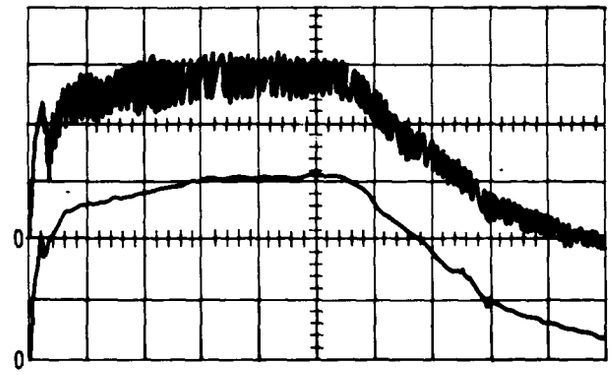

COMBUSTION DRIVER (M_S 8.0)
SWEEP SPEED: 2 MILLISECONDS/DIVISION
VERTICAL SENSITIVITY: 400 PSI/DIVISION

FIGURE 5e

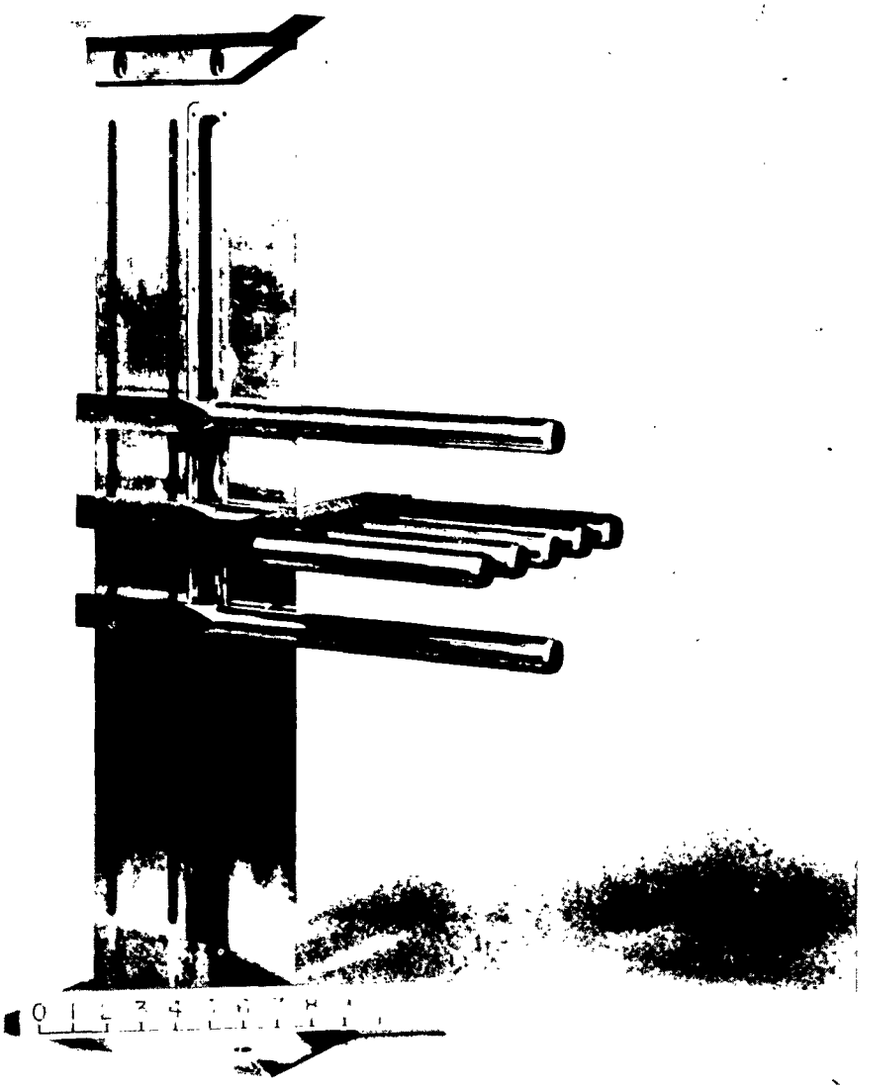

PITOT PROBE STRUT WITH HORIZONTAL CROSS RAKE IN PLACE

FIGURE 6

TYPICAL TEST SECTION OSCILLOGRAMS

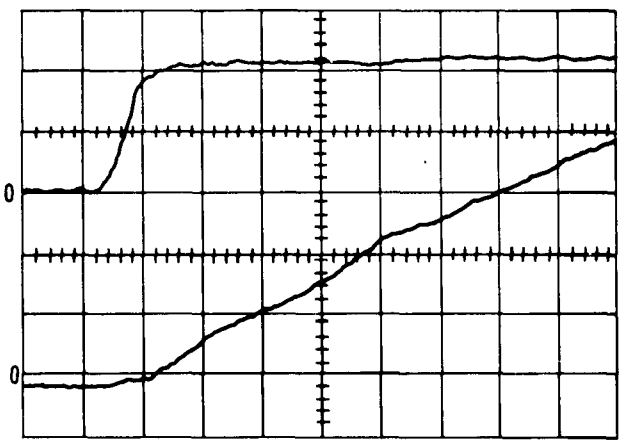

COLD OPERATION WITH 0.840-INCH-DIAMETER THROAT
UPPER: PITOT PRESSURE, 1 PSI/DIVISION
LOWER: CALORIMETER OUTPUT
SWEEP SPEED: 2 MILLISECONDS/DIVISION

FIGURE 7a

TYPICAL TEST SECTION OSCILLOGRAMS

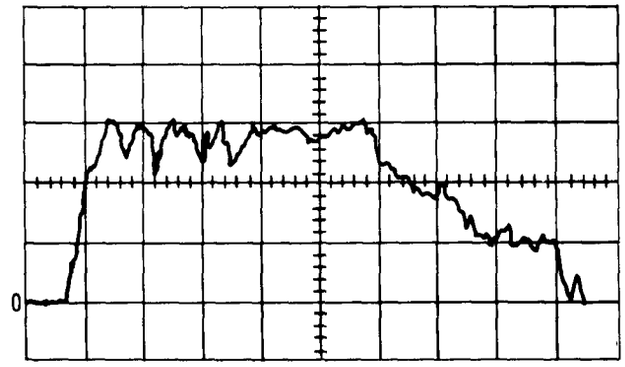

PITOT PRESSURE DURING RUN WITH COMBUSTION DRIVER
SWEEP SPEED: 2 MILLISECONDS/DIVISION
VERTICAL SENSITIVITY: 0.1 PSI/DIVISION

FIGURE 7b

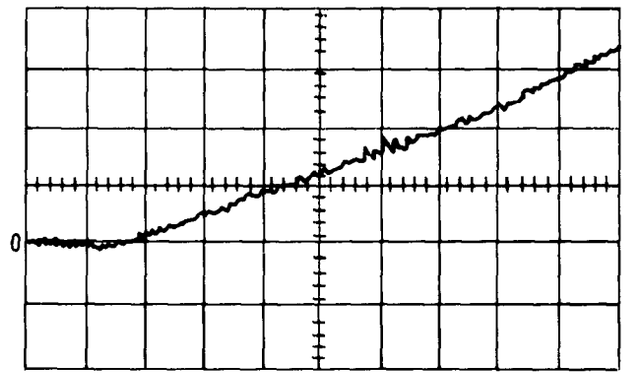

OUTPUT OF CALORIMETER
MEASURING STAGNATION-POINT HEAT-TRANSFER RATE
SHOWING CONSTANCY OF STAGNATION ENTHALPY
DURING EQUILIBRIUM INTERFACE OPERATION
SWEEP SPEED: 2 MILLISECONDS/DIVISION

FIGURE 7c

TEST SECTION VERTICAL AIRFLOW DISTRIBUTION – 0.840-INCH-DIAMETER THROAT, COLD OPERATION

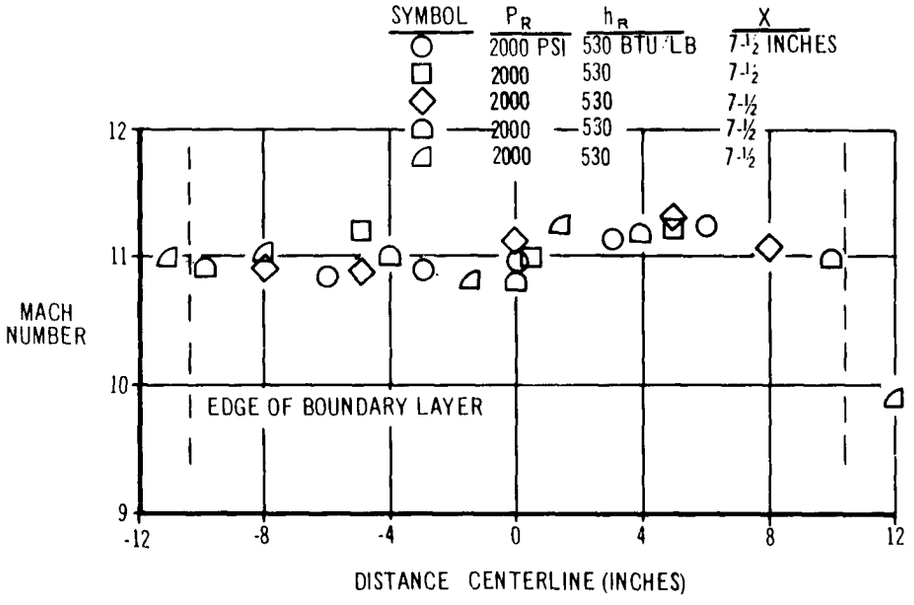

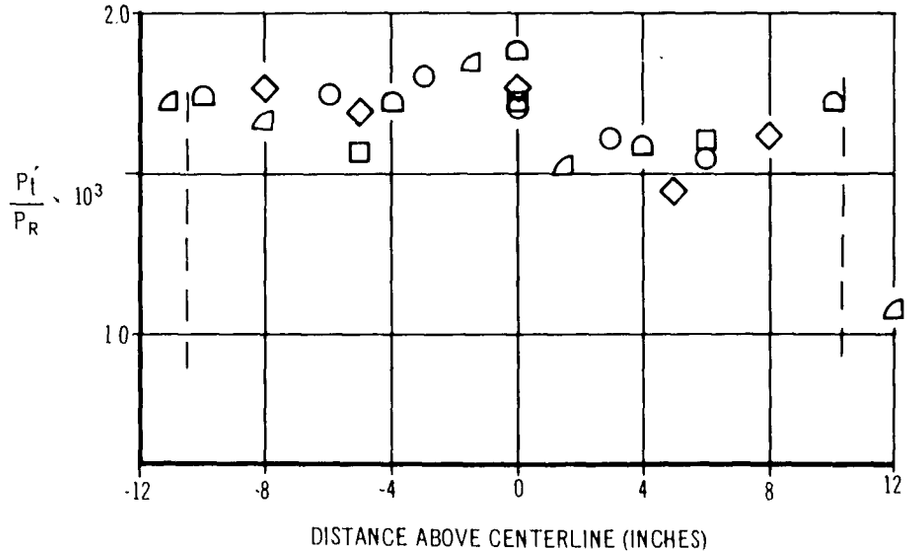

FIGURE 8

VARIATION IN TEST SECTION MACH NUMBER WITH AXIAL POSITION AND RESERVOIR PRESSURE – 0.840-INCH-DIAMETER THROAT, COLD OPERATION

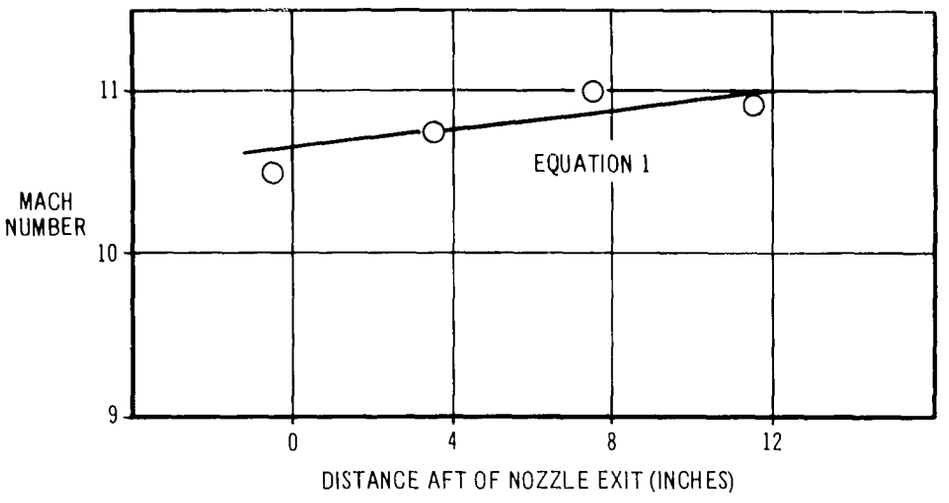

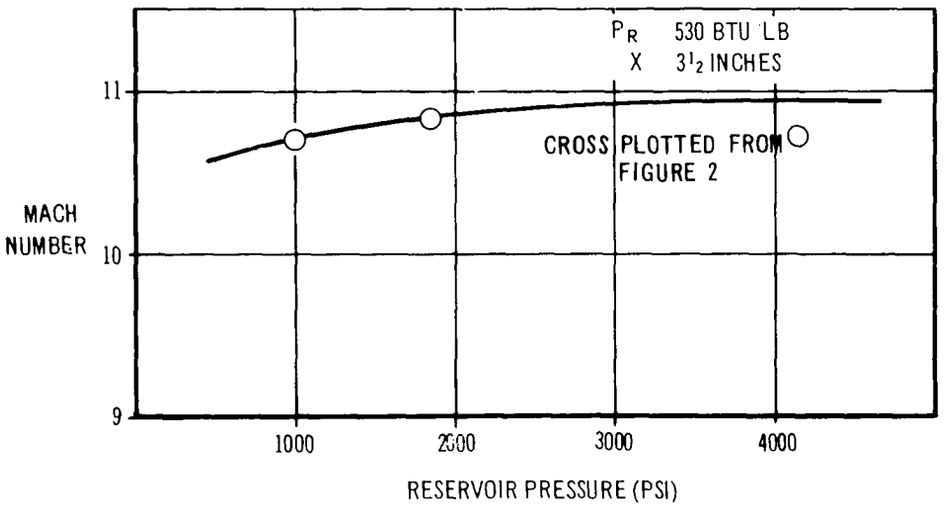

FIGURE 9

TEST SECTION VERTICAL AIRFLOW DISTRIBUTION – 0.840-INCH-DIAMETER THROAT, HOT OPERATION

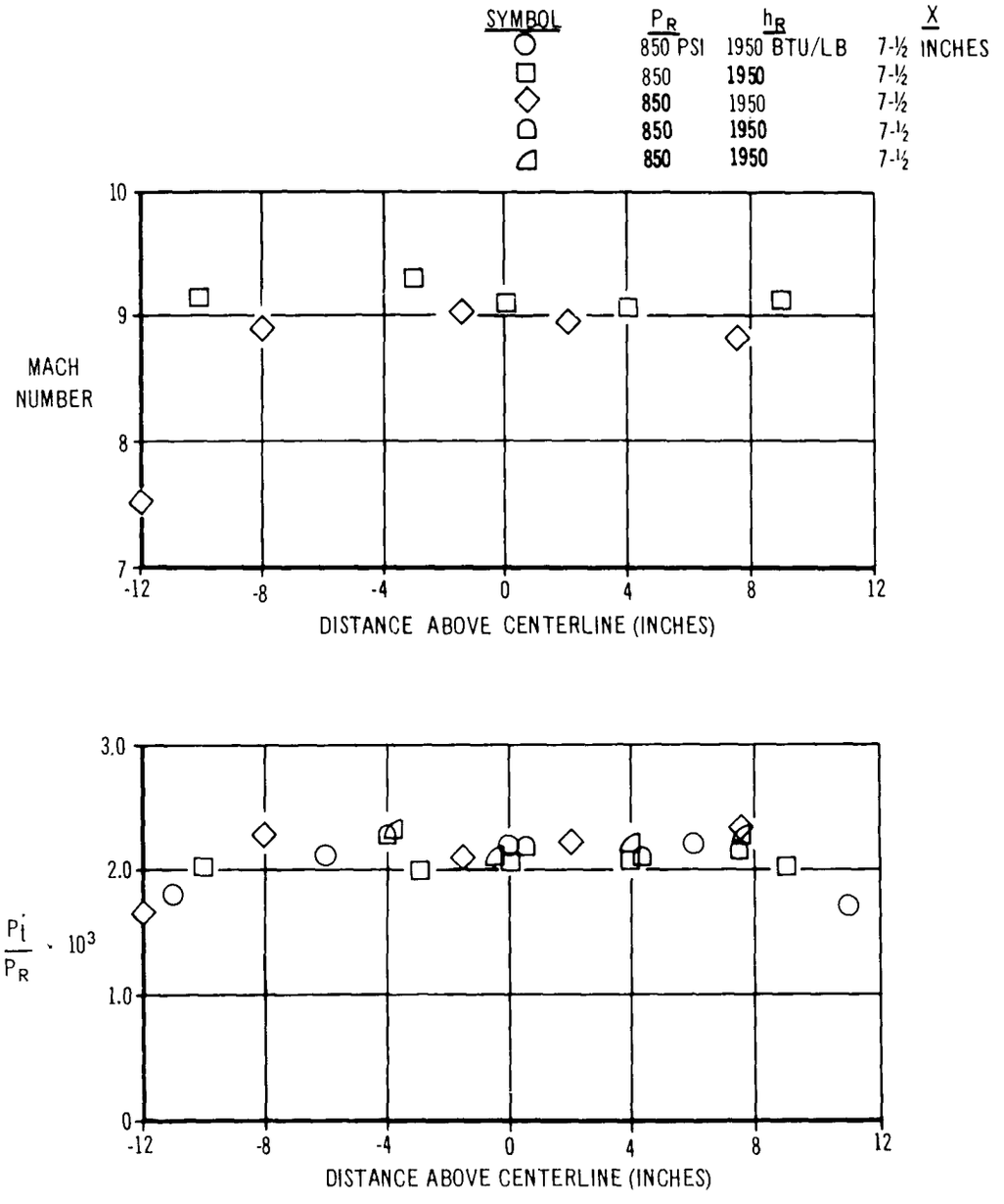

FIGURE 10

VARIATION IN TEST SECTION MACH NUMBER WITH AXIAL POSITION AND RESERVOIR CONDITIONS – 0.840-INCH-DIAMETER THROAT, HOT OPERATION

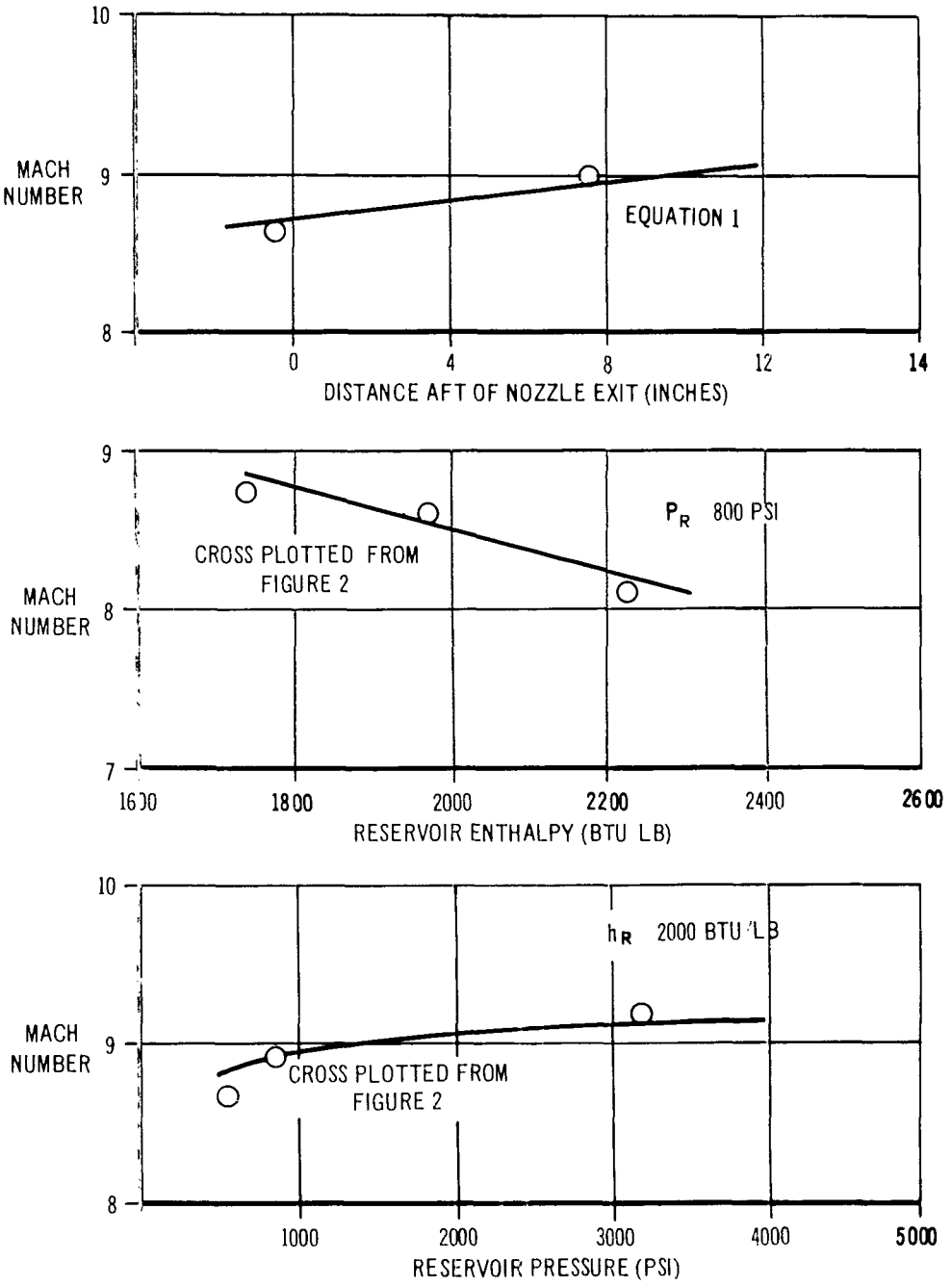

FIGURE 11

TEST SECTION VERTICAL AIRFLOW DISTRIBUTION –
0.120-INCH-DIAMETER THROAT, COLD OPERATION

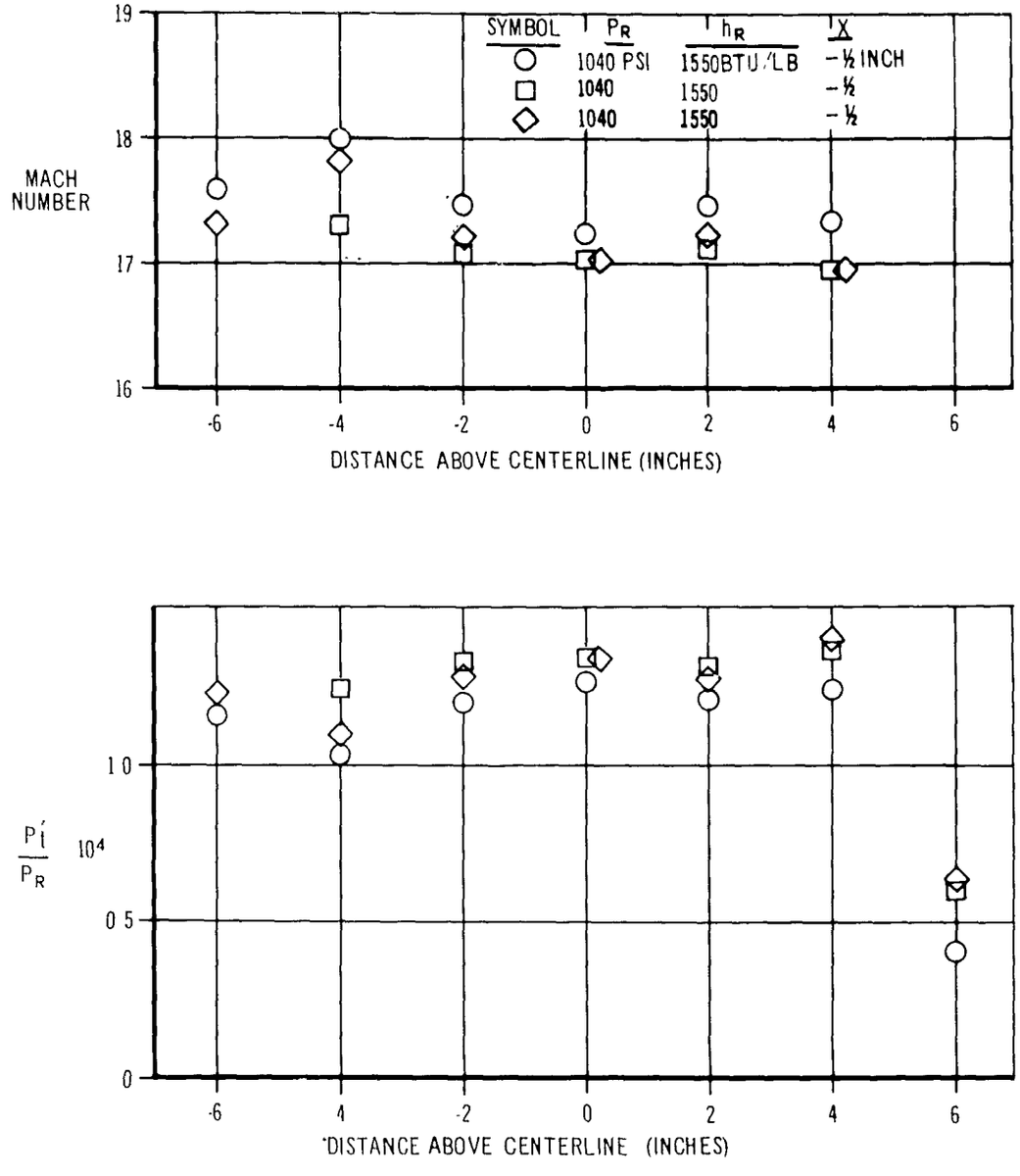

FIGURE 12

VARIATION IN TEST SECTION MACH NUMBER WITH AXIAL POSITION AND RESERVOIR CONDITIONS – 0.120-INCH-DIAMETER THROAT, COLD OPERATION

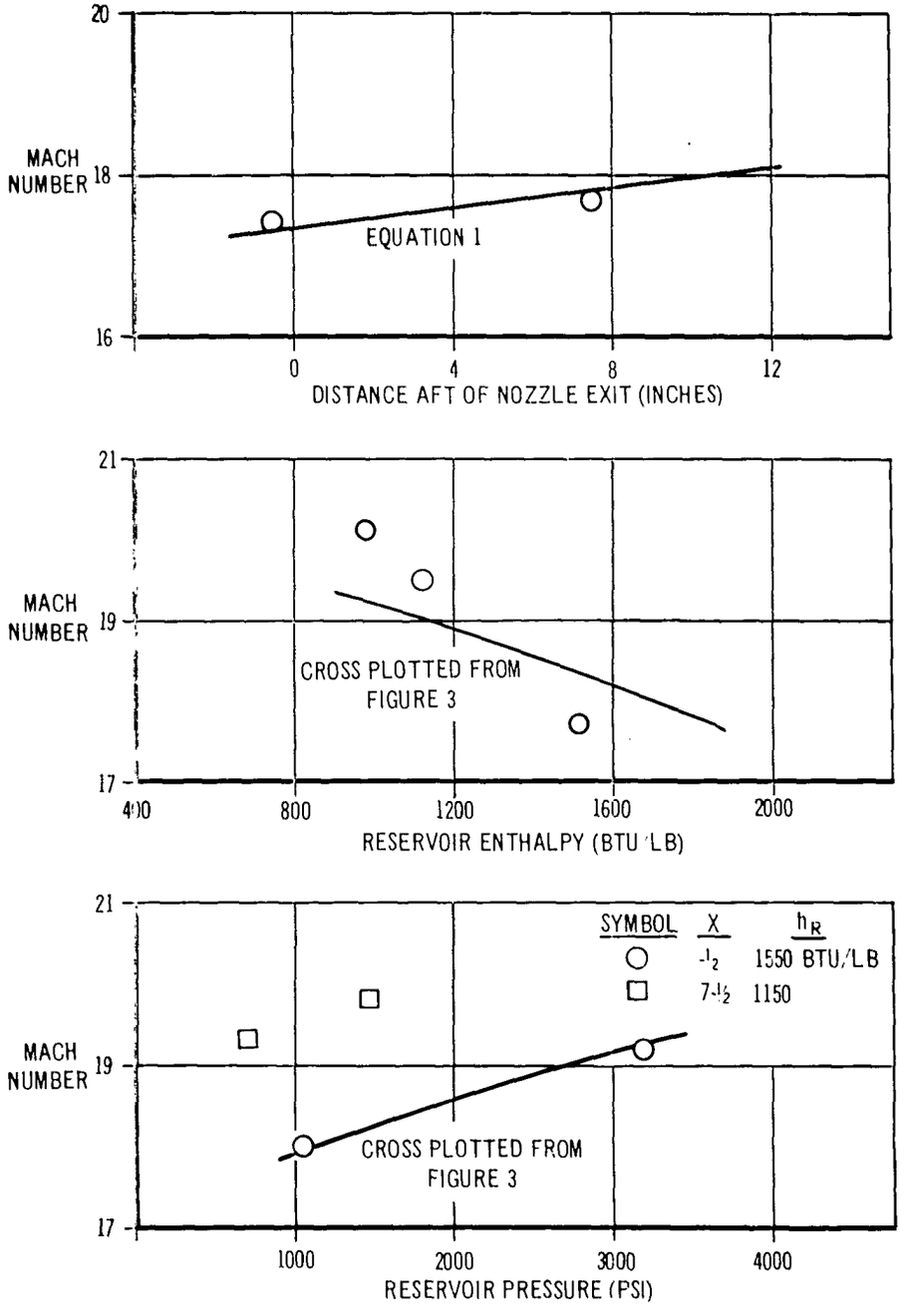

FIGURE 13

TEST SECTION VERTICAL AIRFLOW DISTRIBUTION
0.120-INCH-DIAMETER THROAT, HOT OPERATION

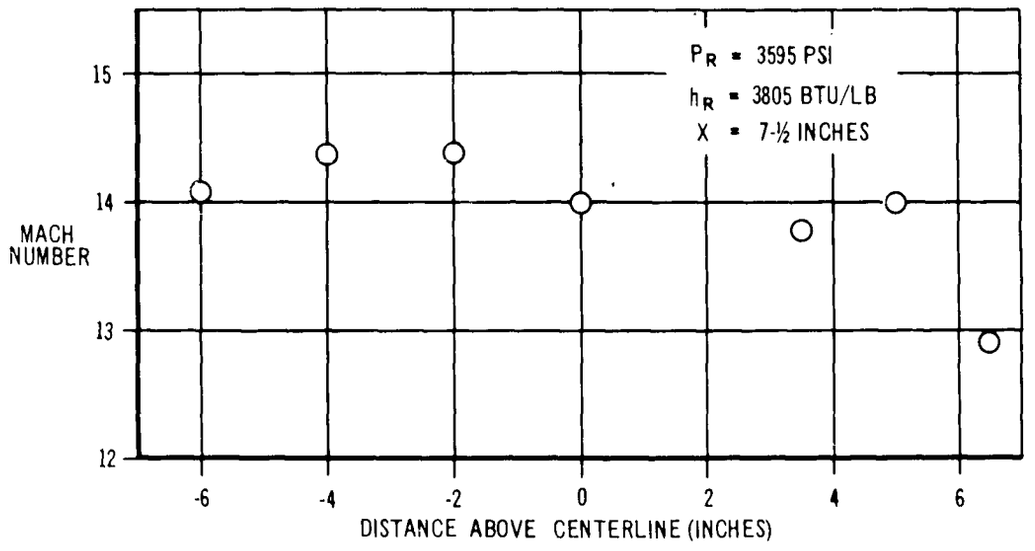

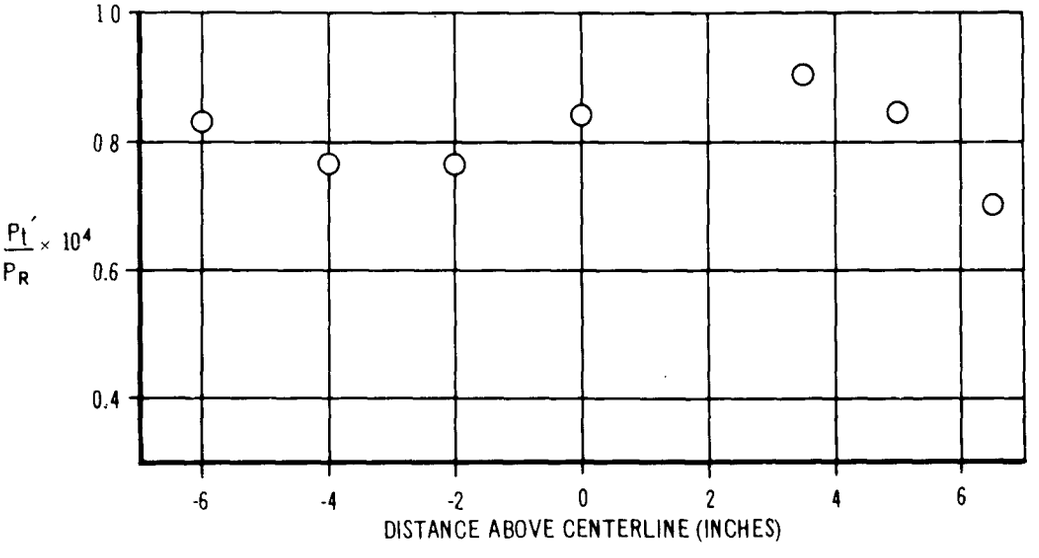

FIGURE 14

VARIATION IN TEST SECTION MACH NUMBER WITH AXIAL POSITION AND RESERVOIR CONDITIONS – 0.120-INCH-DIAMETER THROAT, HOT OPERATION

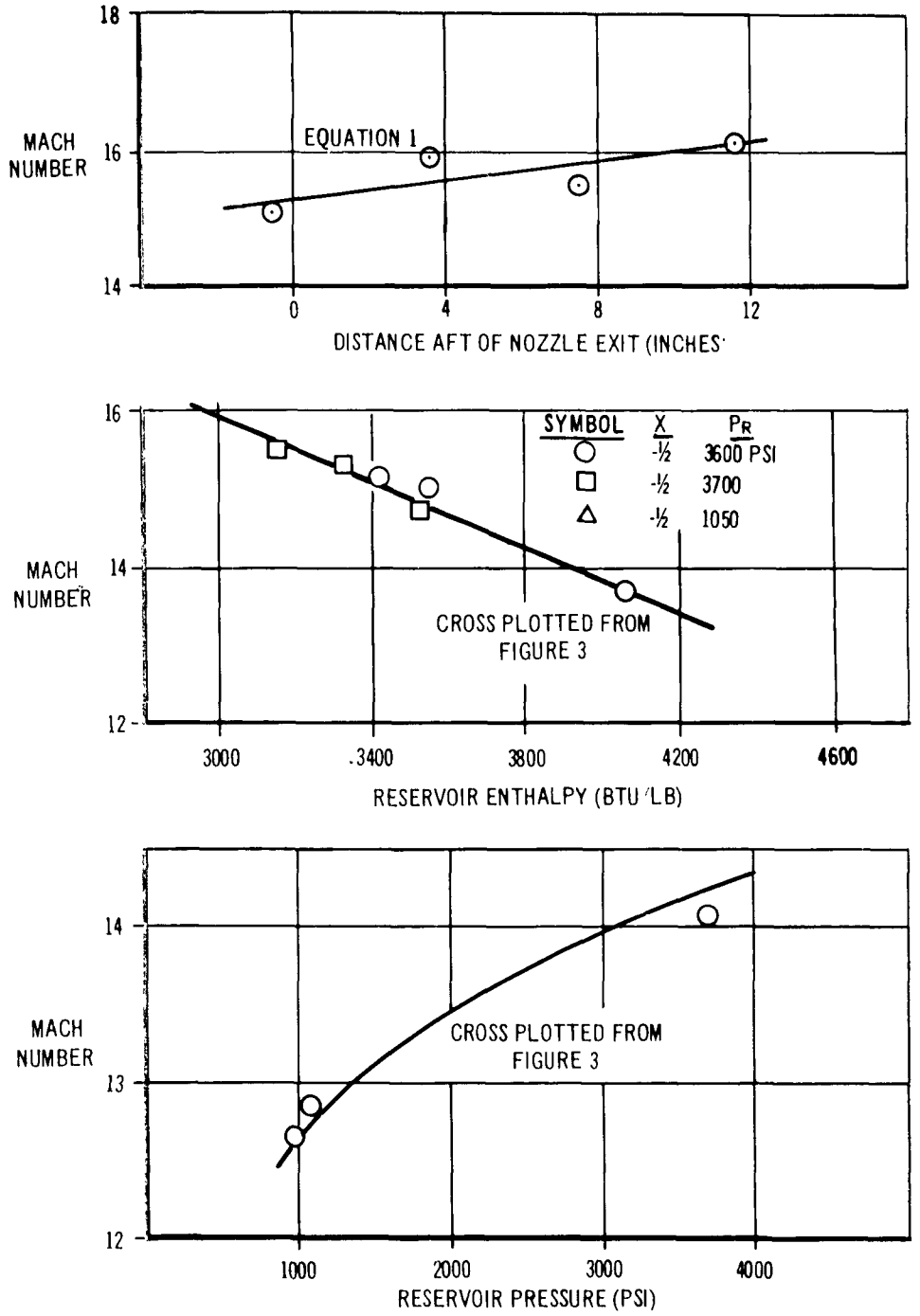

FIGURE 15

TEST SECTION VERTICAL AIRFLOW DISTRIBUTION –
0.030-INCH-DIAMETER THROAT, COLD OPERATION

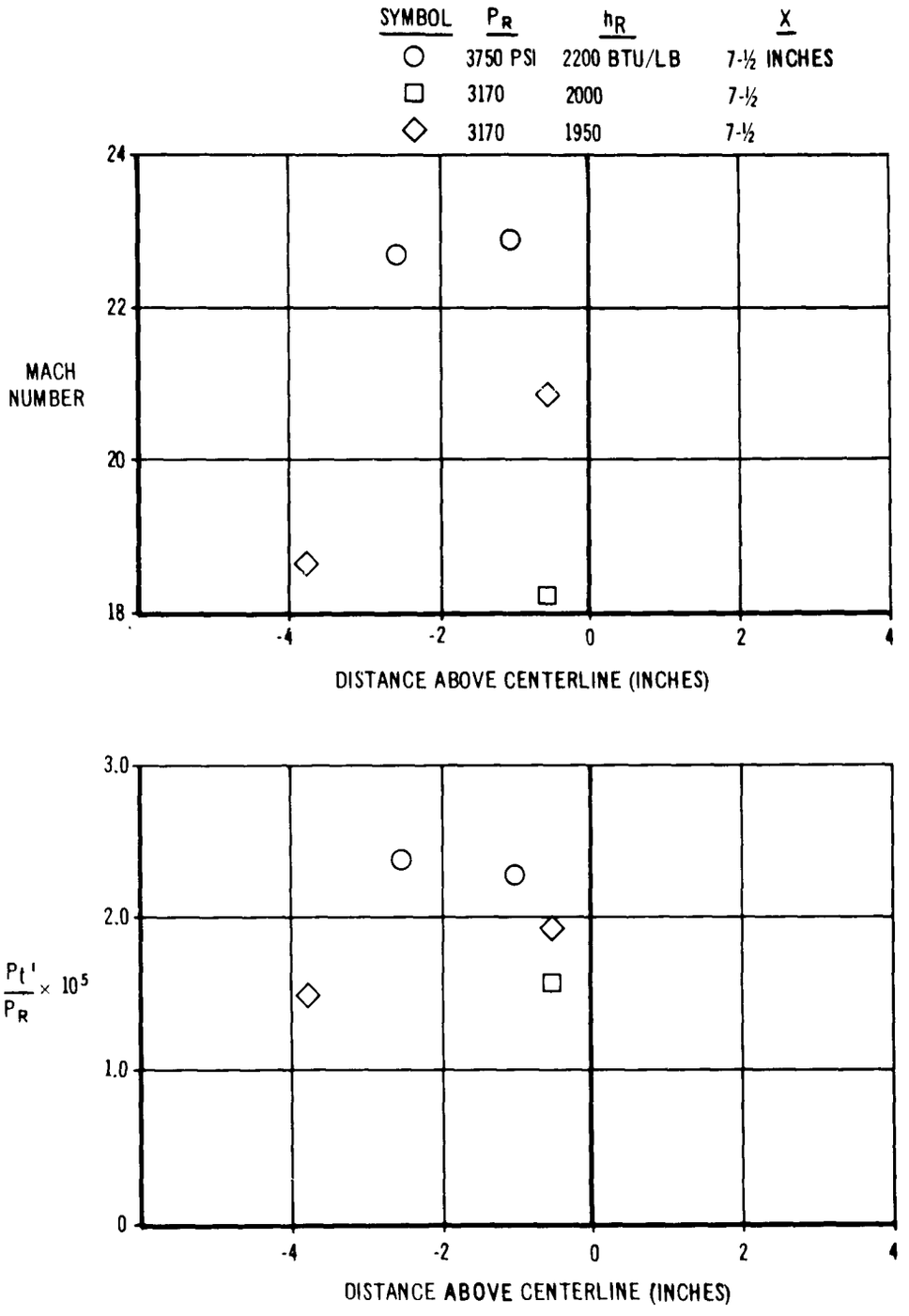

FIGURE 16

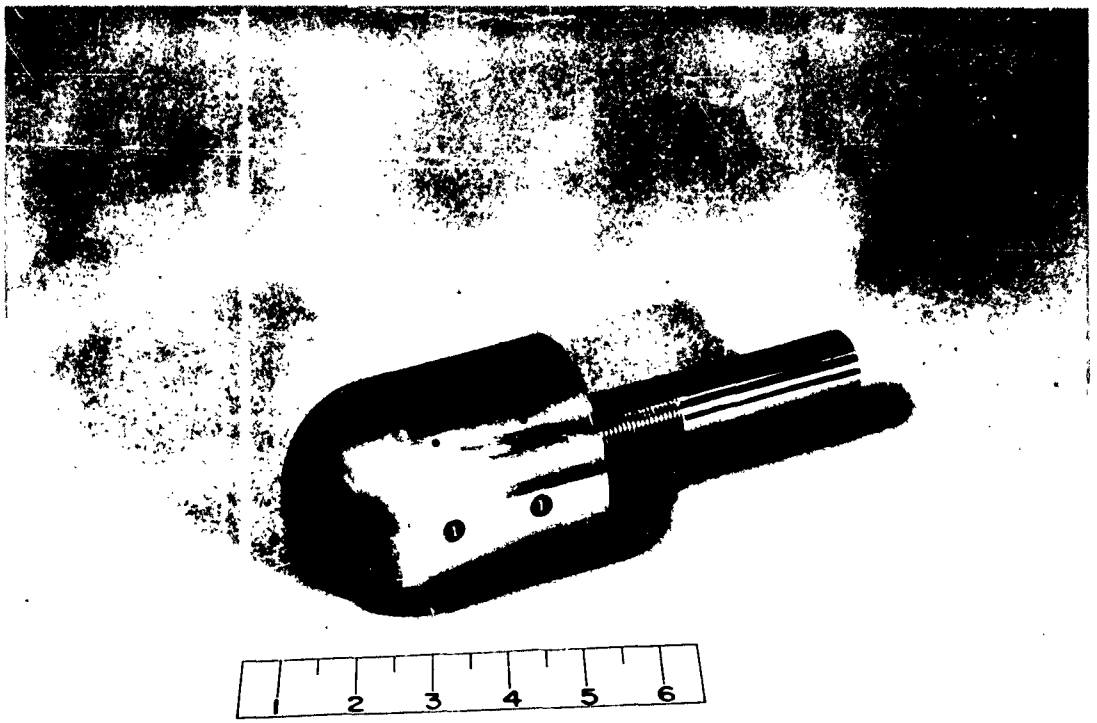

HEMISPHERE-CYLINDER MODEL INSTRUMENTED
WITH PRESSURE TRANSDUCERS AND THIN-FILM RESISTANCE THERMOMETERS

FIGURE 17

TEST SECTION PRESSURE RECORDS OBTAINED WITH
DOUGLAS AEROPHYSICS LABORATORY TRANSDUCERS

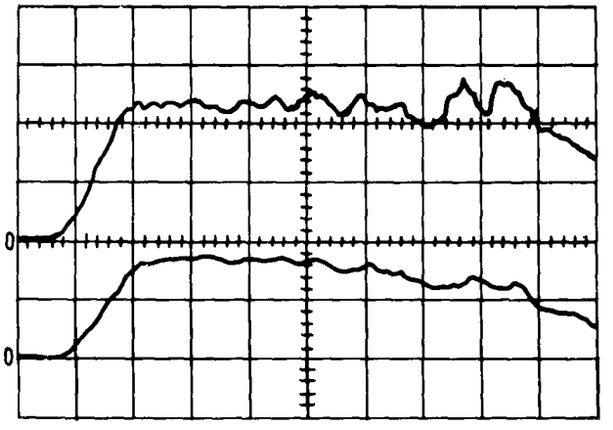

SWEEP SPEED: 2 MILLISECONDS/DIVISION
VERTICAL SENSITIVITY: 0.1 PSI/DIVISION

FIGURE 18

PRESSURE DISTRIBUTION OVER A HEMISPHERE-CYLINDER
OBTAINED IN HYPERVELOCITY IMPULSE TUNNEL
COMPARED WITH OTHER FACILITIES

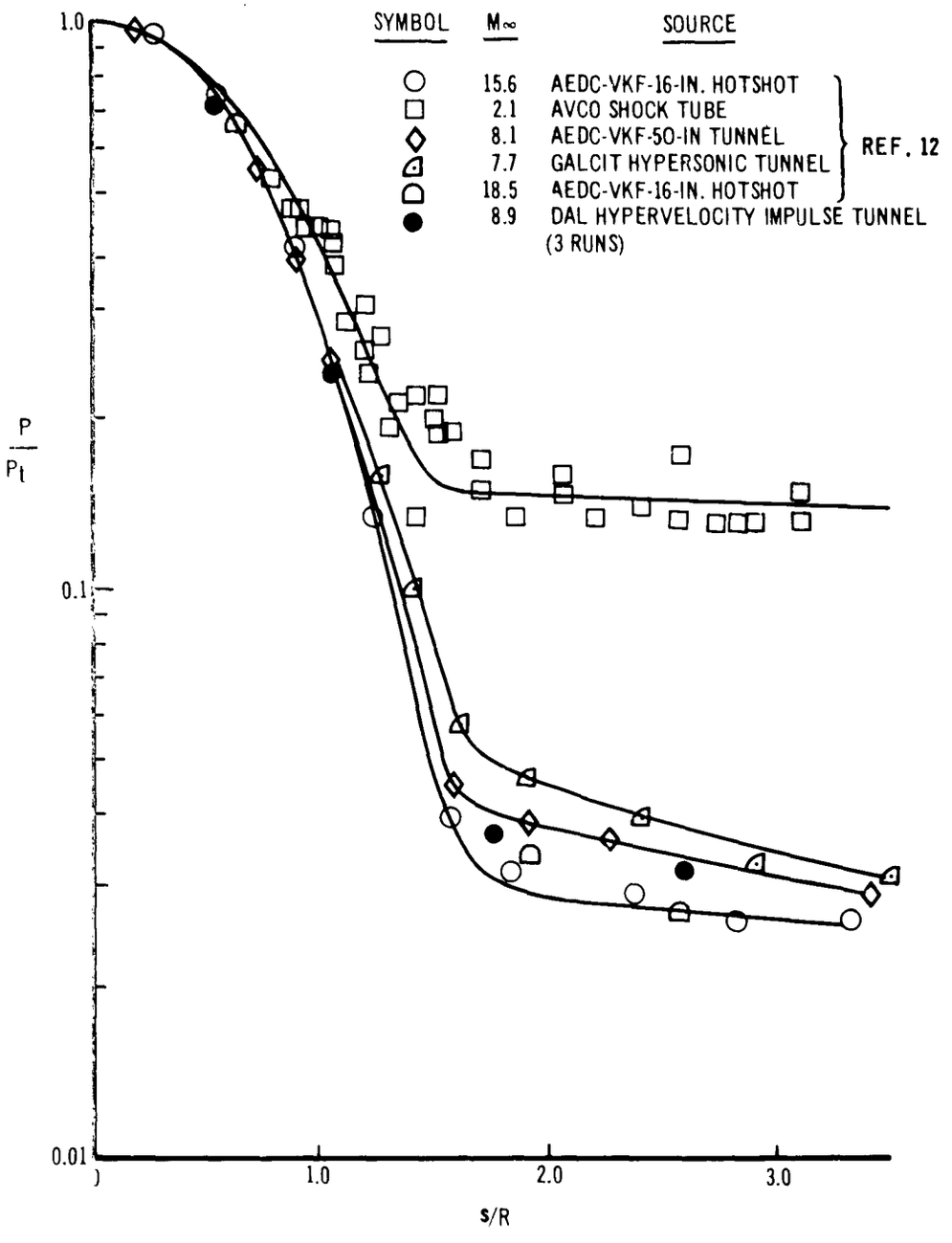

FIGURE 19

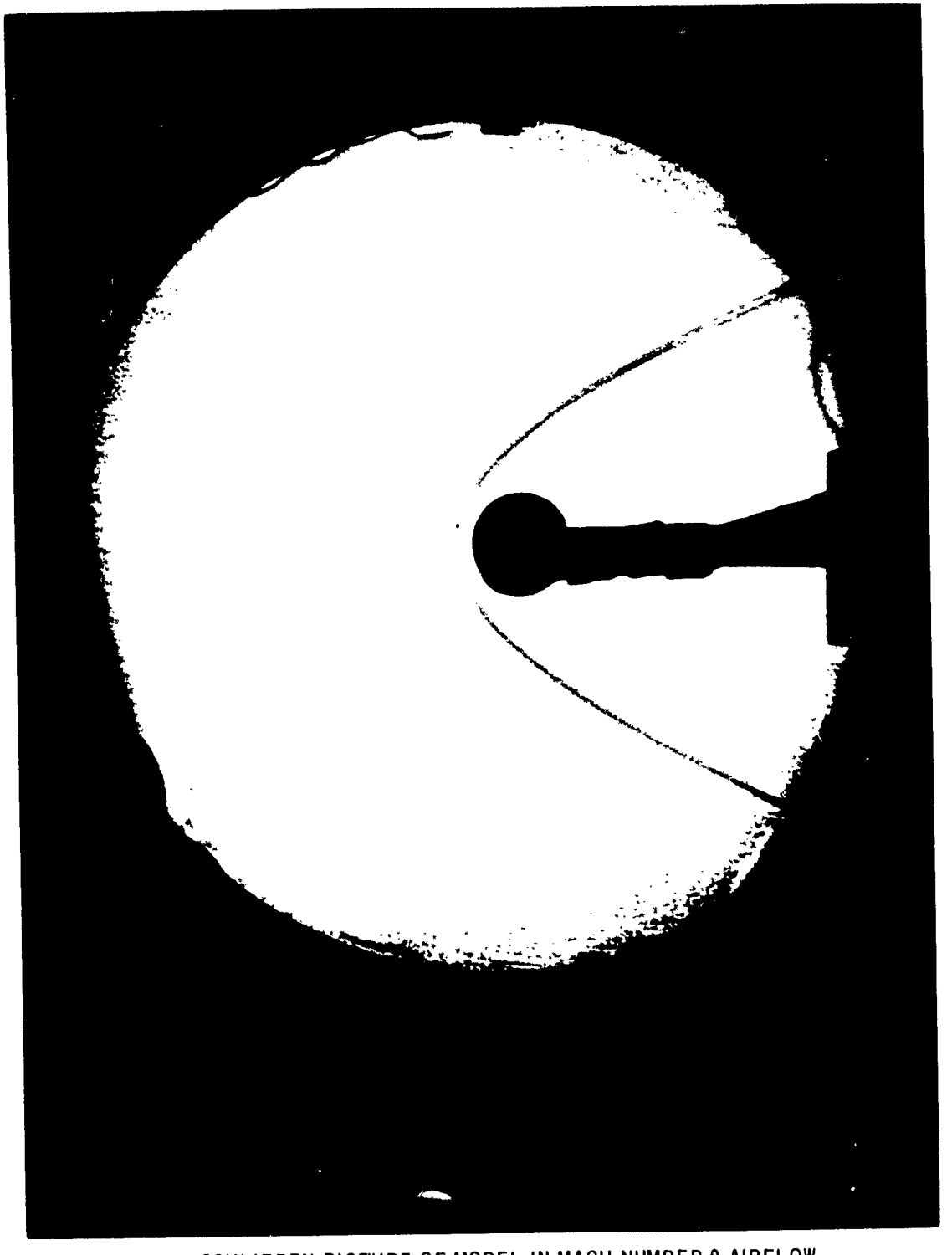

SCHLIEREN PICTURE OF MODEL IN MACH NUMBER 9 AIRFLOW

FIGURE 20

RESISTANCE THERMOMETER RESPONSE

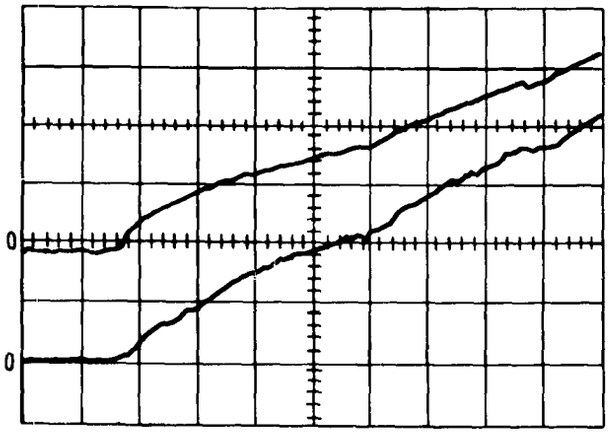

SWEEP SPEED: 1 MILLISECOND/DIVISION
VERTICAL SENSITIVITY: 18°F/DIVISION

FIGURE 21

VARIATION IN HEAT TRANSFER RATE
WITH TIME

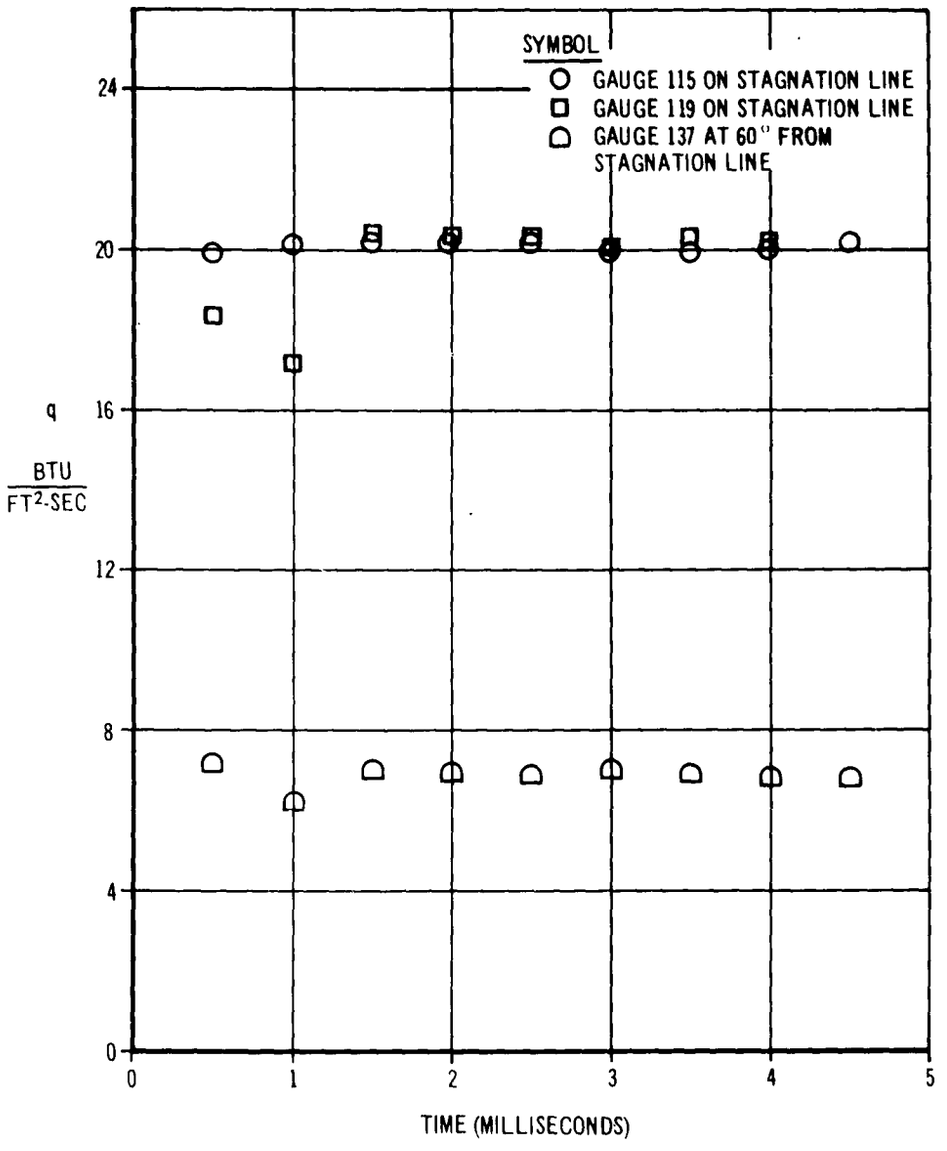

FIGURE 22